

PERIOD CHANGES OF MIRA VARIABLES IN THE M16-M17 REGION

NESCI, ROBERTO¹; SOSZYŃSKI, IGOR²; TUVIKENE, TAAVI³

1) INAF/IAPS-Roma, via Fosso del Cavaliere 100, 00133, Roma, Italy roberto.nesci@inaf.it

2) Astronomical Observatory, University of Warsaw, Al. Ujazdowskie 4, 00-478 Warszawa, Poland
soszynsk@astrouw.edu.pl

3) Tartu Observatory, University of Tartu, Observatooriumi 1, Tõravere, Estonia, taavi.tuvikene@ut.ee

Abstract: We analyzed the light curves of 165 AGB variables, mostly Miras, in the sky area centered between M16 and M17 ($l = 16$, $b = 0$), using the OGLE GVS database in the I_C band. Comparison with the published light curves, derived about 50 years earlier by P. Maffei using Kodak I-N photographic plates, allowed us to find no significant period changes in any star. Remarkably, a few stars of the sample appear to have substantially changed their average luminosity, the most striking case being KZ Ser. We provide a better identification for three stars: IX Ser, NSV 10522, and NSV 10326, all of them being Miras. We classify the light curves of 6 stars, discovered but not classified by Maffei, (GL Ser, NSV 10271, NSV 10326, NSV 10522, NSV 10677, and NSV 10772) five of them being new Miras, and confirm the R CrB nature of V391 Sct. The magnitude scale used by Maffei is compared to the modern I_C one

keywords: Stars: AGB and post-AGB; Stars: late type

1 Introduction

The red Long Period Variables (LPV) are stars on the Asymptotic Giant Branch, in evolution towards the planetary nebula phase. They are historically classified as Mira stars if they have a luminosity variation with a rather regular amplitude and a nearly constant period, or as semiregular (SR) if the amplitude and/or the period is not so regular. Until recently there was no definite numerical threshold to distinguish between these two light curve shapes: a proposal in this sense was made by Soszyński et al. (2013). It is likely that in SR stars at least two periodic oscillations are present, with comparable amplitude, and that their interplay produces their less regular behavior.

An extensive search for the Mira period changes was made by Templeton et al. (2005), based on the large database provided by the American Association of Variable Stars Observers (AAVSO). Out of 547 stars, 21 were found to have definite (greater than 3σ) period changes in one century, the available time extent of good quality light curves. Besides the well known case of T UMi, which is undergoing also a dramatic variation amplitude decrease (Molnár et al., 2019), 7 stars showed secular trends larger than 30 days/century. A similar work by Sabin & Zijlstra (2006) based on the AAVSO and AFOEV (Association Francaise des Observateurs d’Etoiles Variables) datasets for 23 Miras with periods longer than 450 days, showed the existence of small period changes in most of these stars:

generally the period variation is erratic, with differences in a few cases up to 10% on a time interval of tens of years.

With the onset of robotic surveys of very large areas of the sky, very extensive databases containing many kinds of variable stars have been produced. A work by Lebzelter (2011), based on 454 good quality light curves of Mira stars from the ASAS survey¹, discussed the shape of their light curves, finding about 30% of the stars deviate significantly from a simple sinusoid. Both asymmetric shapes and broad maxima exist. The OGLE (Optical Gravitational Lensing Experiment) collaboration (Udalski et al., 2015) has explored the behaviour of late type variable stars in the Magellanic Clouds (Soszyński et al., 2009, 2011) and in the Galactic bulge (Soszyński et al., 2013), providing good light curves in the I_C band, besides the classical V band, and very tight period-magnitude relations. Relevant for this work is the finding that Mira variables have peak-to-peak I_C -band amplitudes larger than 0.8 mag, while SR variables have smaller amplitudes.

In this paper we search for possible period variations at 50 years distance in a set of 165 variables discovered by Maffei (1975), in the years 1967–75, in a 5×5 degrees field centered at $l = 16^\circ$, $b = 0^\circ$. Finding charts and folded light curves of these stars were published only recently in Maffei & Tosti (2013). This field was covered recently by the OGLE Galaxy Variability Survey (GVS), which uses the 1.3-m Warsaw telescope located at Las Campanas Observatory, Chile. The GVS is a subproject of the OGLE survey, aimed at repeatable observations of the Galactic disk and bulge. Currently, the OGLE GVS project monitors brightness of more than one billion stars over an area of about 3000 square degrees. The telescope is equipped with a mosaic camera consisting of 32 CCD chips covering a field of 1.4 square degrees. A detailed description of the instrumentation, photometric reductions and calibrations of the OGLE data are provided in Udalski et al. (2015).

The OGLE GVS observations were taken in the years 2014–2020, allowing to check possible variations in the light curves of our sample stars at a temporal separation of about 50 years. A period change can be easily recognized if the star is a regular Mira: uncertain Miras or SRs have by definition a variable period and/or amplitude. However we studied all the stars of the sample to check for possible misclassifications or actual transitions from Mira to SR and vice versa.

Furthermore, attempting to merge the old Maffei’s and the new OGLE datasets, we tried to transform the magnitude scale used by Maffei & Tosti (2013) into the modern I_C OGLE magnitudes.

We remark that, for the large majority of our stars, no further studies were published after the discovery papers.

2 Historic Maffei’s Observations

The variable stars of this sample were discovered by Maffei (1975) using the Newtonian 122 cm and 65/92 cm Schmidt telescopes of the Asiago Observatory between 1961 and 1975 using photographic plates of I-N emulsion and RG5 filter, fairly reproducing the I_C

¹<http://www.astrouw.edu.pl/asas/>

band (see Section 4). A blue plate (103a-O emulsion) of the field was always taken by Maffei in the same night for comparison, but only a few of these variables were detected also in the blue band, as expected for very red stars.

The periods of these variables were later refined by Maffei, using plates with a nearly identical filter/emulsion combination, taken with the 40/50 cm Schmidt telescope of the Catania Observatory in the year 1980, with a few plates taken in 1983–84, and 1990–91. The finding charts, phase-reduced light curves, periods, epoch of maximum, observed maximum and minimum brightness, were finally published by Maffei and Tosti in 1999 and later put into a digitized catalog (Maffei & Tosti, 2013), available at CDS (Vizier II/320). The number of photometric points was not the same for all stars, ranging from 49 to 143: in this respect the stars belong to two groups: one of 87 stars with a median of 57 observations, and one of 67 stars with a median of 122 observations. Besides the published papers, we found in Maffei’s private library also two unpublished Thesis works (supervisor Maffei) regarding these stars: one by Mario Montalto (La Sapienza University, 1971) and one by Sergio Schioppa (Perugia University, 1983), which permitted correction of some misprints in the periods and light curve classifications. Finally, we found also the tables of the original magnitude measures, which allowed us to perform new period determinations with the same software used for the analysis of the OGLE data.

The variability type was assigned by Maffei on the basis of the light curve shape and amplitude. Overall the stars in the sample were classified as follows: 8 eclipsing stars (E or EA), 2 irregular (I), 111 Mira (M), 14 uncertain Mira (M:), 24 semiregular (SR). For 7 stars Maffei did not give a classification. For 15 stars (including the unclassified ones, the irregulars and most eclipsing stars) Maffei did not give a period. The periods were derived with the Press & Rybicki (1989) software based on the Schwarzenberg-Czerny (1996) method: accuracy for well sampled stars is quoted as a few days in Montalto’s thesis. Some periods however are indicated as uncertain (marked with colon (:)) in Vizier II/320 Table 3).

The coordinates of many stars of our sample were checked by Kato (2001) by comparison with the MSX5C catalog. Later, one of us (Nesci, 2018) checked the coordinates of all the stars comparing the original Maffei’s finding charts with the UK Schmidt IV-N plates and the 2MASS catalog, allowing the correction of a few misprints in the original papers and a better identification of some variables; for three stars we further improved the identification during this work (see Section 3.4 below).

3 Modern OGLE observations and Data analysis.

3.1 Periods of the OGLE light curves.

Light curves for 165 Maffei’s variables were found in the OGLE GVS database, with a typical sampling for each star of about 100 points over a 5-year time span, comparable to that of Maffei’s light curves. The photometric errors were usually smaller than 0.01 mag. A few known eclipsing variables were excluded, as well as a few very poorly sampled stars, giving a final sample of 150 stars.

The periods of these variables and 1σ errors were measured with the Tatry code, which

Table 1: Light curve parameters from OGLE data

SIMBAD ID	2MASS ID	OGLE ID	Maffei ID	Per days	errP days	Epoch MJD	Max mag	Min mag
FZ Ser	18080193-1444151	OGLE-BLG-LPV-258610	M173	243.1	0.4	56939	12.5	15.7
GG Ser	18081103-1434279	OGLE-BLG-LPV-258664	M101	362.1	0.8	56879	10.8	12.2
GH Ser	18082202-1524048	OGLE-BLG-LPV-258711	M030	276.3	0.5	56917	12.1	14.2
GI Ser	18082639-1535119	OGLE-BLG-LPV-258733	M090	252.1	0.5	56963	11.2	14.0
GK Ser	18082549-1418077	OGLE-BLG-LPV-258729	M103	373.1	0.4	57123	13.6	16.1
....

implements the multiharmonic analysis of variance algorithm (Schwarzenberg-Czerny, 1996). The median error of our periods estimates is 0.76 days, with standard deviation of the distribution 0.66 days.

We computed the epoch of maximum and variation amplitude with a simple sinusoidal fit using the Period04 code (Lenz & Breger, 2005), assuming the period given by the Tatry code. The epoch of maximum was used to test the predictions of Maffei’s ephemeris, and the variation amplitude to check for possible major changes in the light curve behaviour, keeping in mind the case of T UMi.

While our paper was nearly finished, the OGLE team published a large catalog of Mira variables found in the galactic bulge and disk, including most of our stars (Iwanek et al., 2022). The periods and amplitudes given in this catalog are consistent with ours within the observational uncertainty: the few discrepant cases will be discussed in the next Section.

In Table 1 we present for each star the SIMBAD name, the 2MASS counterpart, the identifier from the OGLE Collection of Variable Stars (OCVS), Maffei’s number, our period, the formal error, the epoch of maximum, the observed maximum and minimum magnitudes rounded at 0.1 mag. For the stars not present in the OGLE catalog we give the internal identifier of the light curve in OGLE database. A Period=0 or err=0 means no actual measure for lack of enough data. No error is also given for the very short-period variables found.

The full Table 1 in ASCII format is reported after the references.

We remark that for stars with period around one year (350–380 d, about 20 stars) there may be a period ambiguity between one year and half year due to the seasonal gap, which is rather large despite the telescope location in the Southern Hemisphere: this gap is even larger in the historic Maffei’s data.

The histogram of the derived amplitudes for the Mira and SR stars is given in Fig. 1 and shows no difference between these two classes, so that it cannot be used to discriminate between them. The puzzling result of this plot is that nearly all stars have amplitude larger than 0.8 mag in I_C , including those classified by Maffei as SR, suggesting that all of them should actually be considered as Miras according to the simple criterion of variation amplitude ≤ 0.4 mag (Soszyński et al., 2013).

The periods histogram (Fig. 2) shows a little prevalence of longer periods for the stars classified by Maffei as Mira, but the overlap of the two distributions is quite large, again

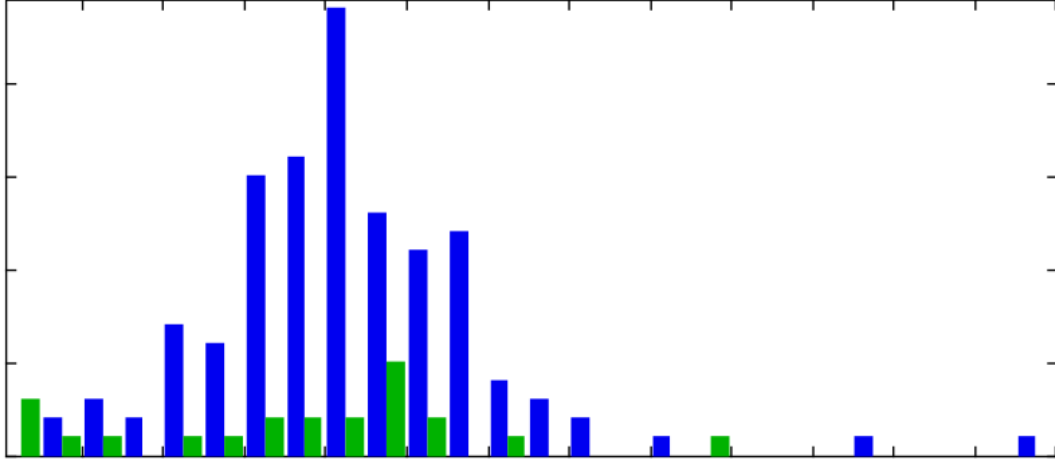


Figure 1: Distribution of variability amplitude based on the OGLE light curves for stars classified by Maffei as Miras and SR variables.

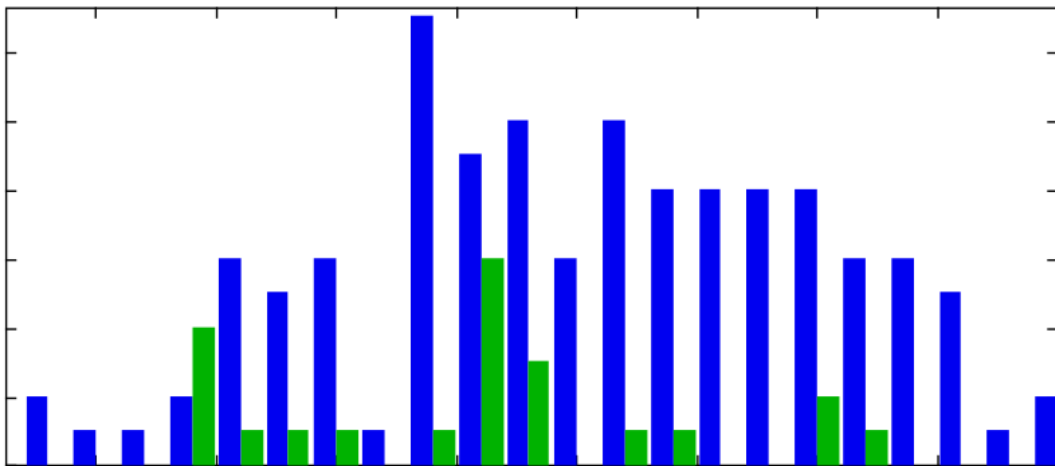


Figure 2: Distribution of periods based on the OGLE light curves for stars classified by Maffei as Miras and SR variables.

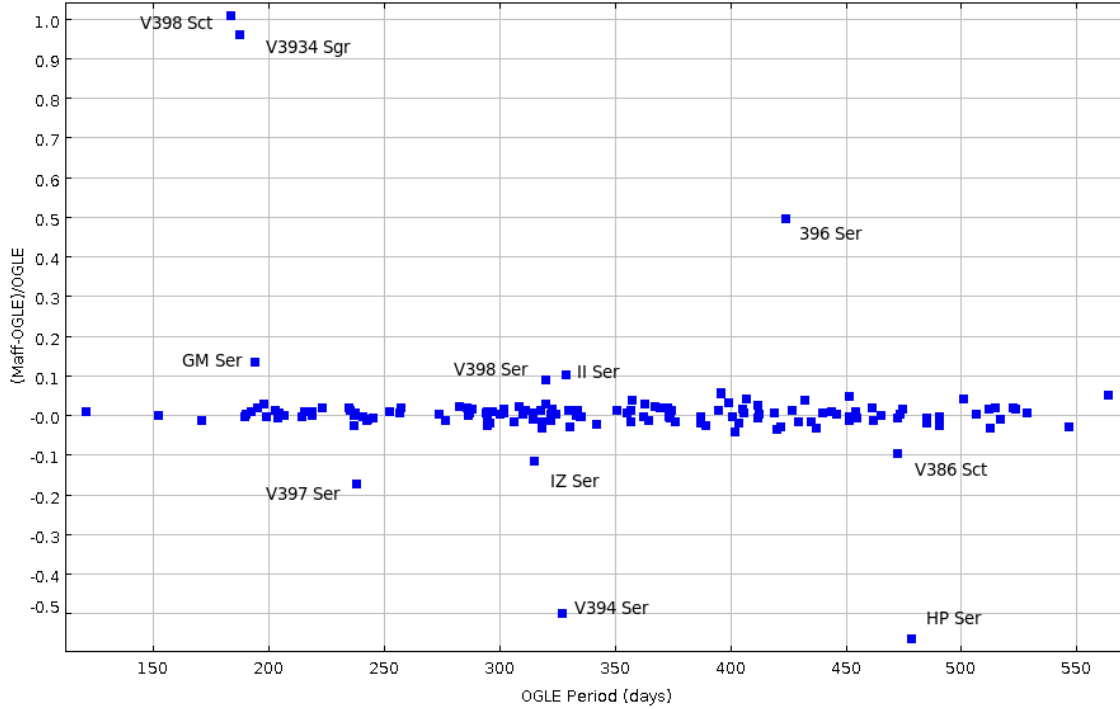


Figure 3: Ratio of the differences between Maffei's and OGLE period to the OGLE period ($\Delta P/P$), vs the OGLE period. Stars that exhibit a large period discrepancy are labelled and discussed in the text.

suggesting a revision of the classification.

3.2 Comparison of Maffei's and OGLE periods.

Having derived the present periods of our stars from the OGLE GVS database, we plot in Fig. 3 for each star the ratio of the difference between Maffei's and OGLE period to the OGLE period ($\Delta P/P$): most of the stars show very consistent results, indicating that no significant period changes happened between the two observation campaigns.

Having found in Maffei's archive his original magnitude measures, we used our Tatry code to derive new period determinations from the old Maffei's observations, to check the effect of using a different code on the period determination: these new period measures were largely consistent with the original ones. Indeed, for a subsample of 129 stars the average difference between the two measures was just 0.21 days (and the median difference even smaller, 0.09 days); the rms scatter was 2.88 days and the maximum period difference found was 13 days, i.e. 5σ . For 6 stars the difference was about a factor 2 or 3, suggestive of period aliases taken as actual periods. For 8 stars the difference was larger than 20 days, anyway below 14% of the period. In 4 cases the Tatry code did not converge to give a Period.

Another way to look for period changes, besides the simple numerical comparison, is to check if the OGLE ephemeris (period and epoch of maximum) predicts correctly the date of Maffei's epoch (or vice versa). The number of cycles for our variables between the

years 1967 and 2014 ranges from about 30 (for a 500 d period) to 70 (for a 200 d period), so that an error of one day (the typical OGLE error) in the period produces a difference of about one to two months in the computed epoch, and a phase difference ranging from 0.06 to 0.28. The accuracy of Maffei's epochs is not declared, and we assume it should be about one week from the shape of a typical Mira light curve.

We made this test computing the expected phase of each light curve at Maffei's epoch, finding a nearly flat distribution between -0.5 and 0.5 instead of a clustering around phase zero as expected if the periods were nearly constant. The same happened computing the expected phase of the light curve at the OGLE epoch using Maffei's ephemeris.

However, given the large number of cycles between the two epochs, a small difference in the adopted period could easily adjust the phase to the nominal value. Indeed we computed for each star an average period, using as time base the interval between Maffei's and OGLE epochs of maxima, and a number of cycles nearest integer to that derived from the OGLE period. Given the very large time base (of the order of 16400 days) and the 365 days length of a typical period, the formal accuracy of these average periods would be about 0.01 days, even if the epoch uncertainty is assumed 2 weeks. If the period were stable, the period computed in this way should be very similar (within a few σ) to the OGLE one, measured on a 4 year time base.

We made this test, finding periods differences $\leq 3\sigma$ for 111 stars, $\leq 4\sigma$ for further 10 stars, and $\geq 5\sigma$ for 14 stars.

As told in the Introduction, fluctuations of a few percent are rather common in Mira variables over tens of years, so we will discuss in detail only the apparently very discrepant stars.

For the large majority (104/111) of the Mira stars the period percent difference ($\Delta P/P$) between OGLE and Maffei was less than 0.04, with rms deviation 0.02, indicating that no significant changes happened in 50 years: only two Miras showed a period discrepant by more than 5%.

Out of the 14 Maffei's probable Miras (M:) only one showed a significant difference.

Out of the 24 SR, two do not have a period by Maffei; three showed a marked period variation ($\Delta P/P \geq 0.5$), whereas three others have $\Delta P/P$ about 0.1. It is remarkable that so many (6/24) stars classified by Maffei as SR have a significantly different period, observed 50 years later, compared with the (2/111) Miras. This may suggest that the criterion to discriminate Miras and SRs just from the light curve amplitude may not be completely sufficient.

Finally, Maffei labelled 8 stars as eclipsing variables, but only 4 have a period reported, always very long, ranging from 196 to 592 days. From their OGLE light curves these four stars are classified as follows: GM Ser is an R CrB star; V374 Sct is a Mira with a period similar to Maffei's one; V382 Sct has only 50 points in OGLE but looks rather irregular; V397 Ser looks a SR. Of the remaining four stars, two are actually short-period eclipsing stars (NSV 10497, $P = 4.11316$ d; NSV 10681, $P = 1.84228$ d); one is a Mira (NSV 10249, $P = 191.5$ d); one looks a SR (NSV 10832, $P = 320$ d).

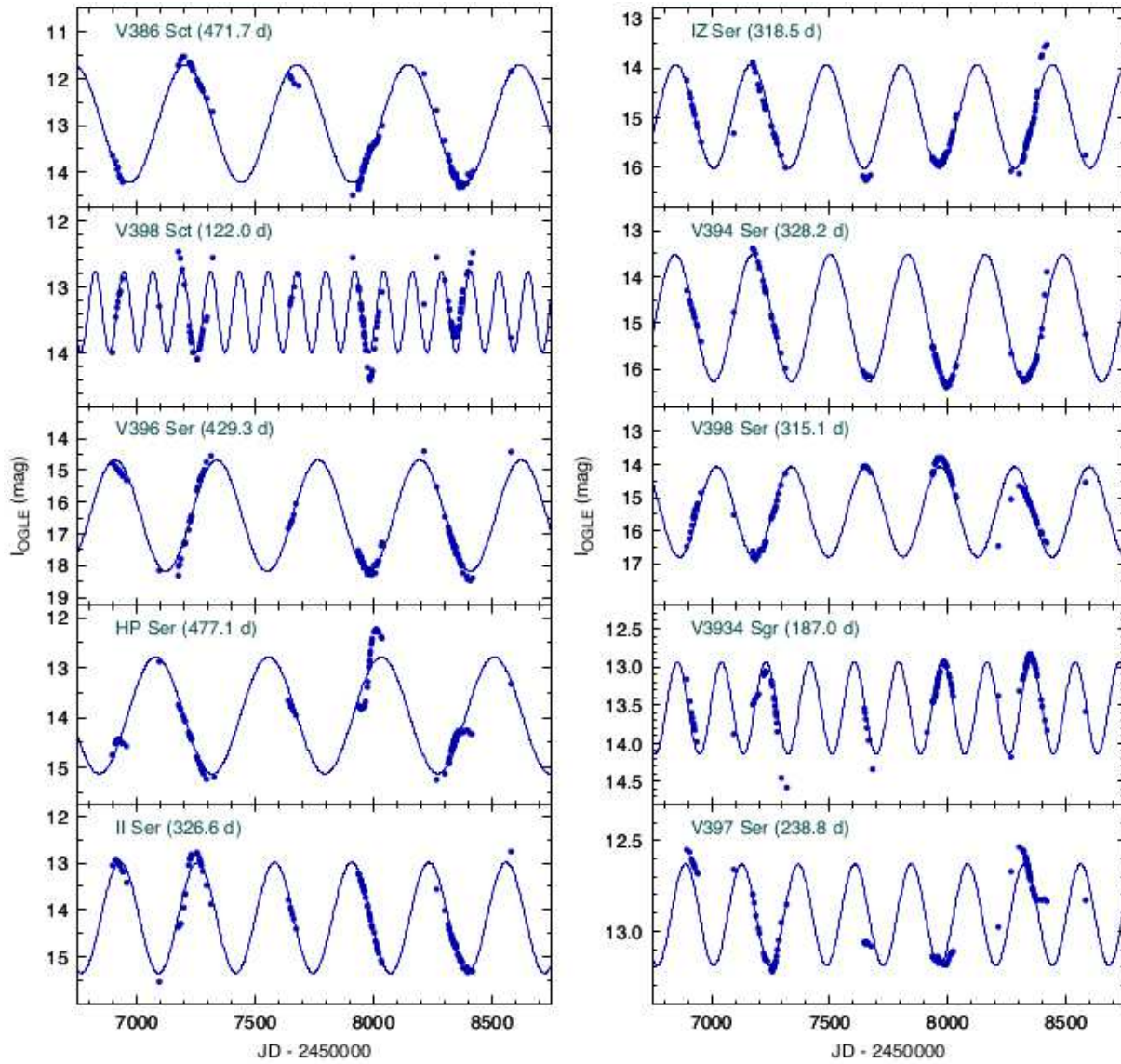


Figure 4: OGLE photometry with fitted light curves for the period-discrepant stars.

Table 2: Stars with discrepant periods

Name	Maffei	OGLE	Cl.	P_{Maffei} d	P_{OGLE} d	errP d	$\Delta P/P$
V386 Sct	M026	OGLE-BLG-LPV-263898	M	426	472.4	1.0	-0.097
V398 Sct	M145	OGLE-BLG-LPV-264150	M	368	183.3	0.4	2.016
V396 Ser	M132	OGLE-BLG-LPV-261077	M:	633:	423.9	1.41	0.474
HP Ser	M093	OGLE-BLG-LPV-259581	SR	208	478.1	1.1	-0.564
II Ser	M041	OGLE-BLG-LPV-259900	SRa	362	328.7	0.8	0.108
IZ Ser	M178	OGLE-BLG-LPV-260964	SR	278	314.8	1.1	-0.127
V394 Ser	M046	OGLE-BLG-LPV-260384	SR	163	326.9	0.4	-0.503
V398 Ser	M186	OGLE-BLG-LPV-264150	SR	348	319.9	1.5	0.104
V3934 Sgr	M109	OGLE-BLG-LPV-262824	SRa	366	187.0	0.4	0.957
V397 Ser	M175	BLG780.16.28126	EA	196	237.8	0.7	-0.179
GM Ser	M092	BLG766.05.11	E	219	193.8	0.8	0.132

3.3 Discrepant stars

The most period-discrepant stars are listed in Table 2, grouped according to the original Maffei’s classification, and their OGLE light curves are shown in Fig. 4. We report in column 1 the SIMBAD name; in column 2 Maffei’s number; in column 3 the OGLE identifier; in column 4 Maffei’s classification; in column 5 Maffei’s period; in column 6 the OGLE period; in column 7 the formal OGLE period error; in column 8 the ratio of the periods difference to the OGLE period ($\Delta P/P$).

We examined more in detail these stars to see if they really underwent a period change, and are discussed below. The interactive code Peranso (Paunzen & Vanmunster, 2016) was used to interactively build phased light curves with different periods and evaluate the significance of the adopted periods.

a) Mira stars.

V386 Sct: its period is indicated by Maffei & Tosti (2013) as 426 d in their Table 3, but as 446 d in their Figure of the phased light curve. We re-measured Maffei’s period with the Tatry code using Maffei’s magnitudes finding 447 d, in fair agreement with the OGLE one. The OGLE light curve is nicely sinusoidal with a small rms deviation and a period of 472 d, so it does not seem a case of significant period change.

V398 Sct: the OGLE light curve shows minima of different depth and a period of half year, while Maffei gives one year. The phase-reduced light curve published by Maffei shows a large spread around the maximum phase. Maffei’s data are not incompatible with the OGLE period (183 d): likely Maffei’s estimate was biased by the seasonal gap and a real period change is not likely.

V396 Ser (NSV 10472): The light curve in Maffei & Tosti (2013) has only 10 points and the quoted period is tentative. The light curve in the OGLE database is well populated and rather regular, with a large amplitude (4.0 mag peak to peak) and a period not compatible with Maffei’s suggestion. It can be classified safely as Mira, but it is not possible to check if a period change really happened.

b) SR stars.

HP Ser: the OGLE light curve shape shows a strong bump in the ascending branch, not uncommon in Miras, with variable level. Maffei's period recomputed with Tatry is 492 d, similar to the 478 d OGLE one, with a difference of just 3%; the variable amplitude of the light curve, and the low accuracy of Maffei's magnitudes makes the 14 days difference not very significant.

II Ser: the OGLE light curve is quite regular, typical of a Mira. Maffei's period is not compatible with the OGLE light curve, but his phased light curve is bad. Our recomputation of Maffei's period with Tatry code gives 3 possible periods of nearly equal weights, one of them similar to the OGLE one: there is no evidence therefore of a period variation.

IZ Ser: the OGLE light curve is well behaved and Mira-like but with variable amplitude. Our recomputation of Maffei's period with Tatry gives the same period of the OGLE data. We remark that using the Lombe-Scargle method on Maffei's original data gives the same result given by Maffei, while for the OGLE data gives nearly the same period of the Tatry code. This difference is likely due to the much larger photometric errors of the photographic magnitudes. Also for this star there is no evidence of period variation.

V394 Ser (alias NSV 10391); the OGLE light curve is well behaved and with a period double of Maffei's one. The phased light curve by Maffei shows several points at odds. Our reanalysis of his data shows several periods of nearly equal weight (164, 226, 328 d), the shortest one being Maffei's one, and the longest one being the OGLE one. Maffei's data are strongly dominated by a dense sampling, 170 days long, made in 1980. Maybe the star was correctly classified as SR by Maffei, but its behavior was quite regular during the OGLE monitoring.

V398 Ser (alias NSV 10479): Maffei's light curve has a small amplitude due to many upper limits; the OGLE period is definitely different from Maffei's one. It shows a large amplitude variation and small phase shifts, so it is likely a Carbon star, not a regular Mira.

V3934 Sgr: the OGLE light curve shows large amplitude variations between consecutive cycles. Maffei's data can be well fitted by the OGLE period or by its double with very similar significance, so there is no convincing evidence of a transition from the fundamental frequency to the first overtone.

c) eclipse star:

V397 Ser (alias NSV 10475): Maffei does not show a phased light curve of this star, classified as eclipse, and its period is flagged uncertain. The OGLE light curve shows a small amplitude (0.6 mag peak to peak) and a quite scattered phased light curve using a 238 d period. The star looks an Irregular or SR variable.

GM Ser: classified as eclipse by Maffei with spectral type M7 (Montalto's thesis); classified as CrB in SIMBAD. The OGLE light curve is well fitted by a small-amplitude sinusoid, but shows a sharp deepening and a small flare, indicative of an R CrB: therefore its light curve is not shown in Fig. 4. Tisserand et al. (2013) have contested its R CrB classification, but confirmed the spectral type M7.

Table 3: OGLE data for Maffei’s unclassified stars

Name	Maffei	OGLE	Period d	Amp. mag	mean I_C mag	Class.
GL Ser	M031	OGLE-BLG-LPV-258777	171	1.23	13.70	Mira
NSV 10271	M174	OGLE-BLG-LPV-258970	300	1.73	14.89	Mira
NSV 10326	M005	BLG766.18.154	315	0.93	15.31	Mira
NSV 10522	M035	OGLE-BLG-LPV-261605	456	1.97	16.19	Mira
NSV 10677	M028	OGLE-BLG-LPV-262404	394	1.13	15.32	Mira
NSV 10772	M183	BLG569.19.104	262	0.12	13.74	SR

3.4 Further remarks

Wrong identifications.

During the present work we found three stars with wrong identification.

NSV 10326 (Maffei M005): no period and classification were given by Maffei for this star. The present identification in SIMBAD is with a blue star, much brighter than the value reported by Maffei; we found a source, at 20 arcsec distance, 2MASS J18110050-1423082, with quite red colors, whose OGLE light curve is typical of a Mira star with a period of 315 days. We therefore identify this star with Maffei’s variable M005.

NSV 10522 (Maffei M035): no period and classification were given by Maffei for this star. The SIMBAD counterpart of M035 was found substantially constant in the OGLE data. We made therefore a new careful comparison of Maffei’s finding chart with the DSS I-band plate available from the STScI and the 2MASS image from SIMBAD, finding a new candidate at 9 arcsec distance, 2MASS J18182915-1725379. The OGLE light curve showed that this star is a large amplitude Mira with a period of 457 days.

IX Ser (Maffei M179): our identification is with 2MASS J18153810-1505332, 9 arcsec off the quoted position in SIMBAD. Its OGLE light curve is typical of a Mira variable, with amplitude and period very similar to those quoted by Maffei (amplitude 1.66 mag, $P=303$ d).

Other variables.

Two stars were classified as irregulars by Maffei and therefore had no period measure. One of them, NSV 10899 (M024, 2MASS J18295552-1518384), has a time scale of 34 days in the OGLE data and we classify it as an RV Tau star. In the OCVS catalog its period is reported as 68 days, double than ours. The second star, V391 Sct, has an R CrB light curve and was already classified as such by Tisserand et al. (2013).

Unclassified stars.

For six unclassified stars of Maffei’s sample we derived the light curve and the period from the OGLE database: we have checked the VSX database to see if they have been studied in detail after Maffei’s publications, finding nothing. Five of them are Mira variables, both from the amplitude and from the period length, and one is a SR; two stars are new identifications, as discussed above. Our measures of periods, amplitudes, mean magnitudes, and classifications for these six stars are listed in Table 3.

Corrections of mistakes.

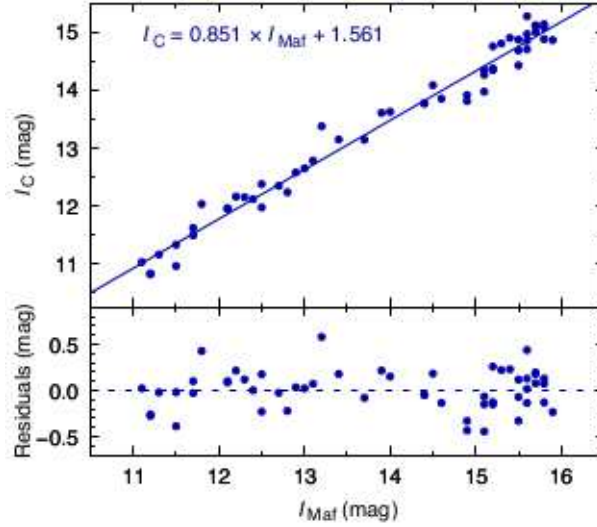


Figure 5: Comparison of the original Maffei's I magnitudes of the comparison sequence with the OGLE I_C magnitudes.

During this work we found two inconsistencies in Maffei & Tosti (2013), which are listed below.

M015, V405 Sct: the period is 307 d in Table 3 but 357 d in the light-curve Figure; in the discovery paper (Maffei, 1975) the period was 362 d. The OGLE value 359.2 d is in agreement with the original value.

M203, V374 Sct: originally classified as SR by Maffei (1975) with 400 d period, and in the thesis work by Schioppa (1983) with 408 d period, from a dataset of 38 points. Later it was reclassified as E in Maffei & Tosti (2013). The OGLE data (110 points) show a Mira variable with 420 d period. Our reanalysis of Maffei's data with Tatry confirms a 409 ± 2 d period: the difference is only 2.6%, not much relevant.

Overall, after our careful analysis, no star among those classified as regular Miras appears to have changed its period by a significant amount.

4 Comparison of the OGLE magnitudes with Maffei's ones.

After checking the periods, we tried to verify if any star had significantly changed its average magnitude or variability amplitude.

As written in Section 2, the filter and emulsion used at the Asiago Observatory to obtain infrared plates were respectively RG5 and Kodak I-N. The RG5 filter is a longpass with cutoff at 665 nm, and the red cutoff is provided by the Kodak I-N emulsion around 900 nm. The plates taken in the years 1980 and following were taken at the Catania Observatory with the 40/50/120 cm Schmidt telescope and RG695 + I-N filter/emulsion combination. According to Bessell (1979) (his Table 7), the Cousins I_C filter can be approximated with photographic material with an RG 695 filter (instead of RG5) in combination with Kodak IV-N emulsion, which is the improved finer grain version of the I-N emulsion. The blue cutoff difference between these two filters is 30 nm, while the width at half maximum of

the I_C filter is 110 nm, so that the bandwidth increase is about 27%. Given that the spectrum of an M-type star is monotonically decreasing blueward within the I_C band, the magnitude difference between the two filter/emulsion combinations is comparable to, or lower than, the errors of Maffei’s magnitudes. Indeed, Maffei & Tosti (2013) did not make any correction when merging the datasets of the two instruments to build their light curves.

Anyway, when Maffei established his magnitude scale in 1967 the Cousins system was still not defined; therefore he established a comparison sequence on the Asiago plates with an approximated Johnson’s I magnitude derived by extrapolating the UBV magnitudes of 60 stars of the Walker (1961) sequence in the open cluster NGC 6611, which is located near the center of Maffei’s field.

We found more details, including the actual list of the stars and their adopted magnitudes, in Montalto’s thesis. Instrumental magnitudes for these comparison stars were derived by Maffei with the Becker iris photometer of the Monteporzio (Roma) Observatory and a calibration curve was built using the above mentioned infrared magnitudes. Secondary comparison sequences were then built by Maffei in selected areas of the field of view, to allow the magnitude estimates of the discovered variables, which were made by eye inspection with a microscope. The internal accuracy of Maffei’s individual magnitudes is reported to be from 0.1 to 0.3 mag (Maffei & Tosti, 1995). We stress that no actual infrared standard stars were used by Maffei, so his scale is not linked to the present Cousins system.

To perform a transformation of the infrared magnitudes of Maffei’s primary sequence (I_{Maf}) into the OGLE I_C magnitudes, we recovered from the OGLE archive the I_C magnitudes of his 60 comparison stars. The scatter plot of these OGLE magnitudes with Maffei’s ones is plotted in Fig. 5, which shows a good linear correlation, namely:

$$I_C = I_{\text{Maf}} \times 0.851(\pm 0.017) + 1.561(\pm 0.239), \quad (1)$$

with rms deviation 0.21 mag. The slope of the regression line is significantly shallower than 1.0, suggesting the existence of some systematic effect: unfortunately the stars of the Walker sequence do not contain very red stars, so that it is not possible to check the existence of a color term in the transformation from I_{Maf} to I_C .

To compare Maffei’s magnitudes of the variable stars with the OGLE I_C ones, we transformed the original Maffei maximum and minimum magnitude of each variable star into I_C according to Eq. 1 and computed the average magnitude $((\text{max} + \text{min})/2)$. These average Maffei magnitudes are compared with the OGLE mean magnitudes (derived from the fit of the light curve) in the top-left panel of Fig. 6. Excluding the 10 most discrepant stars, the best fitting slope is 1.23, significantly different from the ideal case of 1.00, with an offset of about 0.5 mag at the plot center; remarkably, the spread is quite large, with an rms deviation $\sigma = 0.72$ mag from the regression line.

The deviation of the slope from the ideal case, and the offset, might be due to a color term, which we could not evaluate given that the Walker sequence does not contain M-type stars, but it is not a concern to detect a possible large change of the mean magnitude of a given variable at ~ 50 years distance. More of concern is the large dispersion of the data from the regression line.

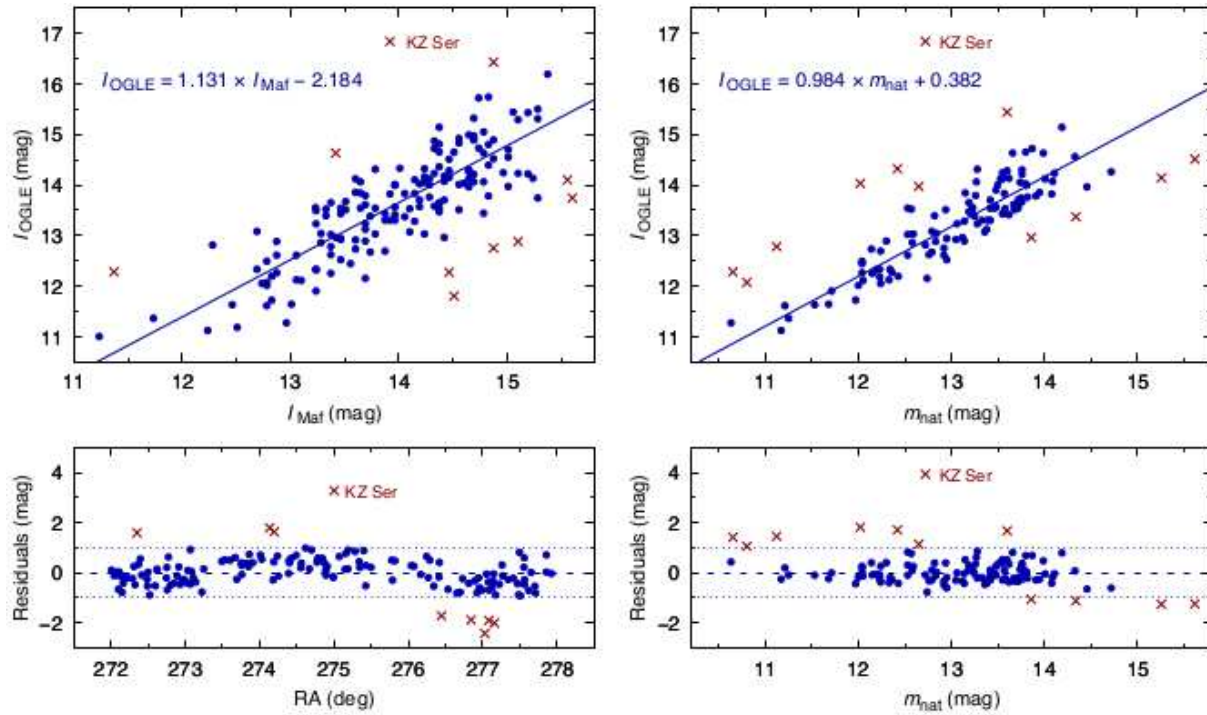


Figure 6: Relations between Maffei's and OGLE magnitudes. *Top left:* OGLE magnitudes of our variables as a function of the mean Maffei's magnitudes transformed into I_C according to Eq. 1. *Bottom left:* residuals of the linear fit as a function of right ascension. *Top right:* I_{OGLE} as a function of mean magnitudes derived from the reanalysed light curves. *Bottom right:* residuals of the linear fit.

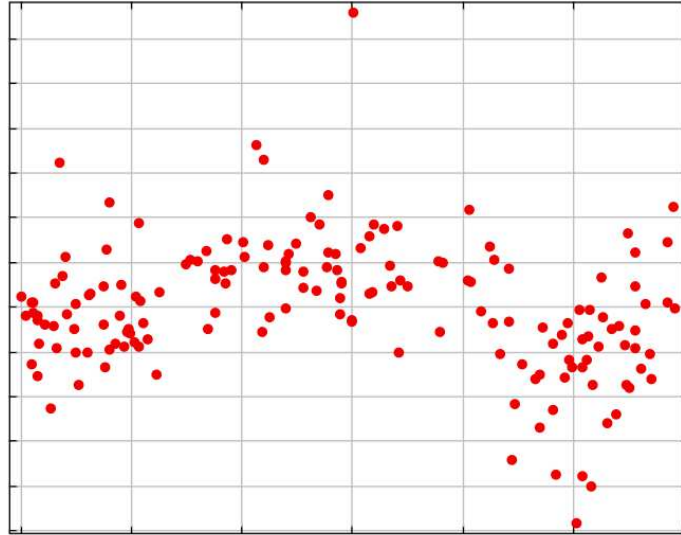


Figure 7: The distance of the OGLE mean magnitude from the regression line of Fig.6 *vs* the R.A. of the star. A systematic trend is present. The very discrepant star at the top is KZ Ser.

A further source of systematic error may be the way of computing the average value: for the OGLE data it comes from the fitting of a sine curve to the whole light curve, for Maffei's data it comes from a simple average of the maximum and minimum reported values.

To understand the reason of the large spread we plotted the magnitude differences as a function of the celestial coordinates, finding a significant trend in RA (see Fig. 6, bottom left). A possible reason of this trend could be inconsistencies among the several secondary comparison sequences actually used by Maffei for his magnitude eye-estimates. For instance, the four outlying stars around coordinates ($l=277$, $b=-2$, see bottom left panel of Fig. 6) have similar declination, so are in the same sky area, suggesting a systematic error in the local comparison sequence.

4.1 Reanalysis of photographic plates

To minimize the systematic errors expected from the inconsistencies of the secondary comparison sequences and from the way of computing the average magnitudes of the variable stars, we reanalyzed 47 Maffei's plates, obtained with the Asiago 65/90 cm Schmidt telescope, and digitized at 1600 dpi (1.59 arcsec/pixel). The astrometric solutions and photometric reductions were carried out using the PyPlate software, in a pipeline developed for the APPLAUSE project (Tuvikene et al., 2014).

The pipeline processed the digitized plate images in multiple steps. Instrumental magnitudes (MAG_AUTO) of all detected sources were extracted with the SExtractor program (Bertin & Arnouts, 1996). Initial astrometric solutions were derived with the Astrometry.net software (Lang et al., 2010) and refined astrometric calibration in sub-fields was obtained with SCAMP (Bertin, 2006), using reference coordinates from the UCAC4 cata-

log. The source list was then cross-matched with the UCAC4 and APASS DR9 catalogs. The typical internal error of the individual PyPlate measures was 0.15 mag, quite comparable to that of the original Maffei's measures, and was basically dictated by the quality of the hypersensitized I-N plates, but in some cases it was up to 0.3 mag. Further details of the procedure can be found in Nesci et al. (2018).

Photometric calibration was carried out with the Sloan r' and i' magnitudes of a large number of non variable stars taken from the APASS DR9. Each photographic plate has a unique color response that can be characterized with the color term C , as explained by Laycock et al. (2010). Magnitudes in the plate natural system, m_{nat} , are related to the standard magnitudes:

$$m_{\text{nat}} = i' + C(r' - i'). \quad (2)$$

We determined the color term for each plate by trying a series of C values to minimize the scatter in the photometric calibration curve. The color terms varied from -0.26 to -0.04 , with a mean value of -0.15 . All instrumental magnitudes were then transformed to natural magnitudes: these m_{nat} are our best estimates of the Sloan i' magnitudes of the individual observations of our variables. Conversion into the I_C band could in principle be made using the formulas by e.g. Jordi et al. (2006) or Jester et al. (2005), but these formulas contain color indexes, which are not known for our variables. The expected approximate zero point difference can be evaluated comparing the m_{nat} magnitudes of the stars in the Walker sequence with their I_C magnitudes in the OGLE database: the comparison was quite satisfactory, with

$$I_C = m_{\text{nat}} \times 1.008(\pm 0.005) - 0.353(\pm 0.081). \quad (3)$$

At first order therefore an offset of -0.35 mag should be expected. As told above in Section 4, the Walker sequence does not contain M-type stars, so possible further color term corrections for the magnitudes of our (very red) variables could be present but cannot be quantified.

Unfortunately PyPlate was in trouble for star images near the plate limit, so for many variable stars our light curve is not well populated. Anyway we were able for 128 stars to compute the mean magnitude and the variation amplitude from the sinusoidal fit of their light curve, derived in the same way as for the OGLE light curves described above in Section 3.1. Despite the actual light curves of our stars are not strictly sinusoidal, the use of the same shape for the OGLE and the Asiago data minimize systematic differences. For stars detected only during the high state, the light curve is not constrained in the faint part, so the mean magnitude and amplitude derived from the sinusoidal fit are less reliable.

For the 118 best sampled stars (good number of points well distributed in phase), the mean magnitude is compared with the OGLE one in the top-right panel of Fig. 6. The regression line shown has slope near unity and the magnitudes offset is negligible. The spread of the stars around the regression line ($\sigma = 0.61$) is reduced with respect to the plot of Fig. 6 (left), made using the original Maffei's data. This is an indication that the systematic errors due to the secondary Maffei's comparison sequences, and to the way of computing the average magnitudes, have been reduced, but remains significantly larger than the nominal accuracy of the individual measures.

Table 4: Stars with possible change of the average magnitude.

Name SIMBAD	OGLE id	Maffei id	I_{OGLE} mag	Period d	ΔI mag	N. of plates
KZ Ser	OGLE-BLG-LPV-261988	M140	16.84	511.9	3.94	13
V414 Sct	OGLE-BLG-LPV-264442	M137	15.44	546.7	1.67	34
V3924 Sgr	OGLE-BLG-LPV-261845	M096	14.32	362.8	1.71	14
V374 Sct	BLG787.23.49	M203	14.03	421.4	1.82	23
V3927 Sgr	OGLE-BLG-LPV-261965	M097	12.78	218.4	1.45	38
GR Ser	BLG767.28.8	M164	12.28	234.9	1.41	45
V383 Sct	OGLE-BLG-LPV-263764	M061	13.97	295.5	1.14	33
V3947 Sgr	OGLE-BLG-LPV-263995	M060	12.07	308.1	1.06	41
V386 Sct	OGLE-BLG-LPV-263898	M026	12.86	472.4	-1.06	29
V398 Sct	OGLE-BLG-LPV-264150	M145	13.37	183.3	-1.12	38
GS Ser	OGLE-BLG-LPV-259041	M020	14.51	373.9	-1.24	25

The most distant stars from the best fit locus are marked in Fig. 6 and listed in Table 4 in order of mean magnitude difference.

We have checked the light curves of these stars to see if an uneven sampling could produce a strong bias. The stars above the line (positive delta mag) are all detected only around the tip of the light curve from the Pyplate pipeline, so their computed average values are unreliable. The stars below the line (brighter than OGLE in the Asiago plates) are poorly sampled with the plates available to us. After careful examination of the light curves we conclude that only two stars have a reliable difference in their mean magnitude, KZ Ser and GR Ser.

The most striking case (4 mag deviation) is that of KZ Ser. This Mira variable has one of the longest period of this sample: the variability amplitude (about 3 mag) is very similar in both datasets, as well as the shape of the light curve, with a very steep rising branch and a long decreasing branch. To check our result we found in the STScI archive two digitized infrared plates (N emulsion) of the Second Palomar Sky Survey (POSS-II) survey, taken on 1980-08-29 (MJD 44480) and 1982-04-18 (MJD 45077): the first plate is simultaneous to a Maffei’s plate taken at the Catania Observatory, while there are no plates around the second date.

At the first POSS-II plate epoch the star was near its minimum (phase 0.77) according to Maffei’s ephemeris: Maffei & Tosti (2013) report a magnitude $I_{\text{Maf}}=16.0$ which is converted to $I_{\text{C}}=15.2$ according to Eq. 1), in fair agreement with the GSC2.3 catalog (15.8). On the second POSS-II plate the star was at phase 0.92, on the steep rising branch, so its expected magnitude is rather uncertain. On the POSS-II plate the star was about 15.4, somewhat brighter than in the first plate, in fair agreement with the expectation. The POSS-II plates therefore confirm Maffei’s observations, so we think that the luminosity drop of ~ 4 mag of KZ Ser detected by OGLE is real. A possible explanation for the star fading may be extinction by a recent dust emission.

GR Ser had a brighter average magnitude at the time of Maffei’s monitoring. It is covered by only one public POSS-II plate (taken on 1980-08-29), simultaneous to a

Maffei's one, with $I_C=10.88$ in the GSC2.3 catalog. Maffei's value is 11.3 (rescaled as above), in fair agreement. The OGLE magnitudes range from I_C 9.5 to 16, while Maffei's monitoring ranged from 10.1 to 13.0 (rescaled according to Eq. 1). Overall the maxima are fairly consistent, so we guess that the different average value is due to the deep minimum detected by OGLE and missed by Maffei.

5 Infrared colors and distance estimates

Our variables are located around galactic coordinates $l = 16^\circ$, $b = 0^\circ$. From the map of the galactic plane by Reid et al. (2014) we expect that they belong to the Scutum and the Sagittarius arms so may be largely spread in distance from 1 to 4 kpc. They may therefore suffer of different absorptions, of the order of 1 to 3 mag in V , or even more.

Having identified a 2MASS counterpart for all our Long Period Variables, we build their $(J - H)$ vs $(H - K)$ diagram (see Fig. 8) where we reported also the loci of Late Type Stars as defined by Bessell & Brett (1988) (their Fig. A3). The 2MASS passbands are not exactly those used by Bessell & Brett (1988), but our purpose is just to check an overall consistency and the presence of significant reddenings. In this plot the continuous line at the bottom left is the Main Sequence, which separates around spectral type M0 into a Red Giants (upper) and a Main Sequence (lower) branch. The area enclosed by hatched lines is mostly populated by variable Carbon stars; that enclosed by the continuous line is populated by Oxygen-rich Long Period Variables. To help the reader, we report in this figure also the reddening vector for $E(B - V) = 1$, computed according to Schlegel et al. (1998).

As expected, all our stars are located in or above the area of the Long Period Variables. Color corrections corresponding to $E(B - V)$ ranging from 1 to 3 mag are required to bring all our stars within the borders of the Oxygen-rich stars locus (continuous line). A discussion of the individual reddening is beyond the purpose of this paper: JHK magnitudes averaged over the full light curve should be necessary, instead of the single snapshots given by the 2MASS catalog.

We searched for a distance estimate of our stars in the Gaia DR2 database (Gaia Collaboration, 2018) as available at CDS: in all cases a matching source with very red $BP - RP$ color was found within 0.35 arcsec from the 2MASS position.

Unfortunately, reliable parallaxes are not available for any of our stars, because the parameters indicating the goodness of the astrometric solution (`astrometric_gof_al`, `astrometric_excess_noise`, `astrometric_weight_al`) are all very poor (Gaia DR2 Documentation, 2019). No parallax accuracy improvements for our stars were given in the EDR3 version (Gaia, 2020). The formal median parallax of our sample is 0.15 mas with nearly symmetric and large spread ($\sigma = 0.59$ mas), many stars having formally negative parallax. The median proper motions of the sample are -2.26 mas/yr in RA and -4.38 mas/yr in Dec, corresponding to -5.0 mas/yr in Galactic longitude and 0.0 mas/yr in Galactic latitude, in fair agreement with the expectations given their positions in the sky.

Assuming the period-absolute K mag relation of Whitelock (2012) and a color excess $E(B - V) = 1$, we get a median distance for the sample of 3.7 kpc, in fair agreement

with the expectation. An accurate distance determination for each star would require a knowledge of the individual reddening and of the actual mean K magnitude instead of the 2MASS snapshot value, which is taken at an unknown phase.

6 Conclusions

The large majority of the 150 Long Period Variables in Maffei's M16-M17 sample show a substantially stable period at a distance of 40–50 years. The original classification as Mira or SR is not supported by the extensive work by Soszyński et al. (2013) on the Red Variables in the Galactic bulge, which sets as discriminating parameter a "peak to peak" amplitude $\Delta I_C \leq 0.8$ mag. In this respect nearly all the LPVs of the sample should be considered as Miras, save three (V397 Ser, NSV 10832, and NSV 10772); increasing (somewhat arbitrarily) the limit ΔI_C to 1.0 mag brings the potential number of SR to just 8 stars, against 24 of the original classification.

A statistical comparison can be done with the finding by Templeton et al. (2005), who studied 547 Mira or possible Mira (M:) stars from the AAVSO database: none of those stars is included in our sample. In the AAVSO sample, only 3 stars showed a period variation larger than 10%: no surprise that we found no star with a significant period variation in our sample of 150 stars.

Regarding the average magnitudes of the LPVs observed by Maffei, they are well correlated with the OGLE mean magnitudes, with a linear relation of slope nearly 1. However, the spread around this relation is quite large ($\sigma = 0.61$ mag), substantially larger than the typical photographic photometry error. It is therefore possible that a few stars have actually changed their mean luminosity by 1 to 2 magnitudes: the most relevant case, with a ~ 4 mag dimming, is KZ Ser.

During this research we found the right identification for 3 misidentified Maffei's variables (NSV 10326 alias M005, NSV 10522 alias M035, and IX Ser alias M179), which will allow their study in the future.

Finally, we point out the reclassification as Mira of five stars in Maffei's sample (GL Ser, NSV 10271, NSV 10326, NSV 10522, NSV 10677), not recognized as such in the original discovery papers.

Acknowledgements: Part of this work was supported by institutional research funding IUT40-2 of the Estonian Ministry of Education and Research. TT acknowledges the support by the Centre of Excellence "Dark side of the Universe" (TK133) financed by the European Union through the European Regional Development Fund. This work has made use of data from the European Space Agency (ESA) mission *Gaia* (<https://www.cosmos.esa.int/gaia>), processed by the *Gaia* Data Processing and Analysis Consortium (DPAC, <https://www.cosmos.esa.int/web/gaia/dpac/consortium>). Funding for the DPAC has been provided by national institutions, in particular the institutions participating in the *Gaia* Multilateral Agreement. This research has made use of the WEBDA database, operated at the Department of Theoretical Physics and Astrophysics of the Masaryk University. We thank dr. Corinne Rossi for helpful suggestions.

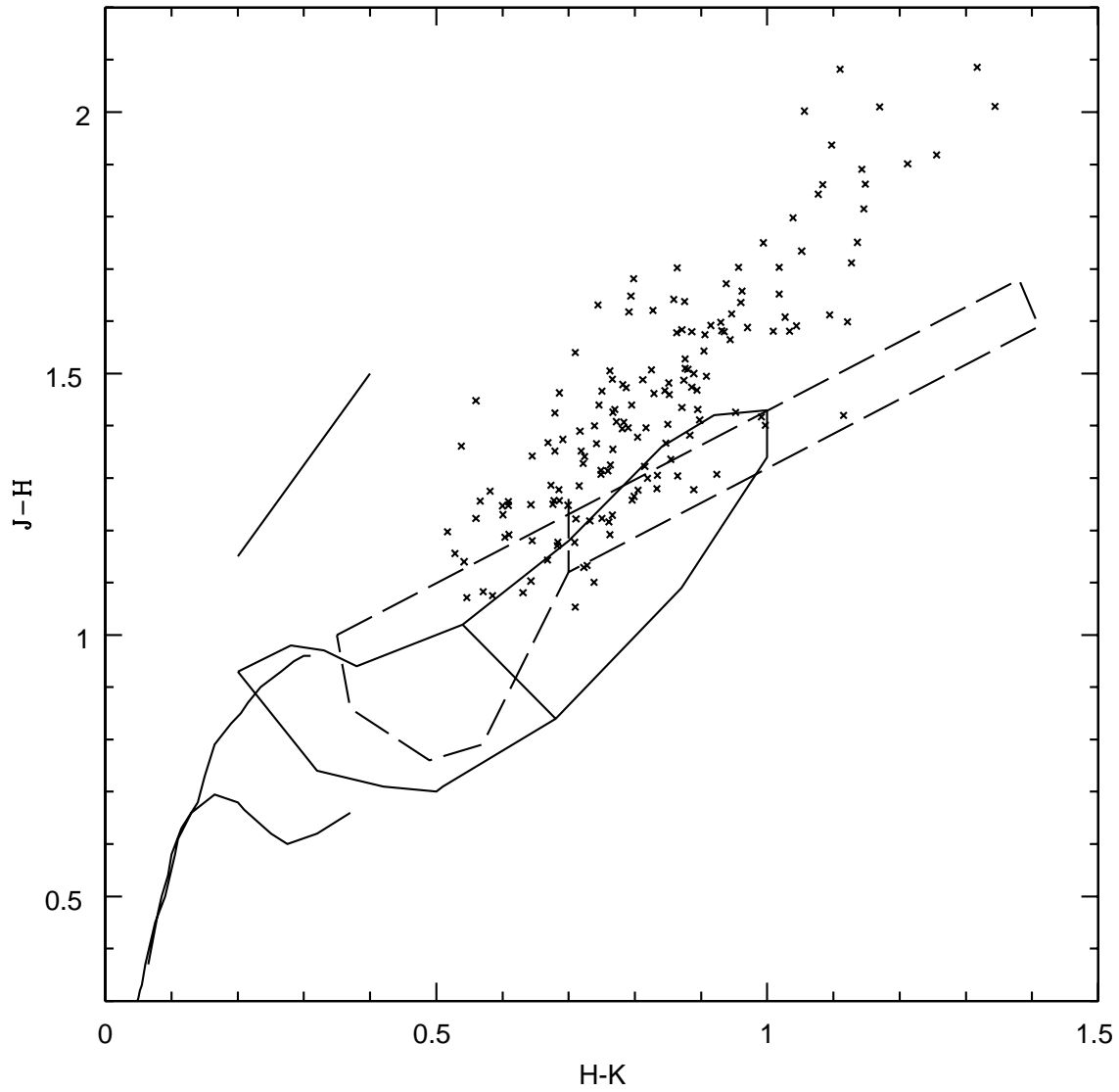


Figure 8: The NIR color-color plot of Maffei's LPVs with an OGLE period overplotted to the Bessell & Brett loci for Late Type Stars described in the text. The reddening vector for $E(B - V) = 1$ is drawn to help the eye.

References

- Bertin, E., & Arnouts, S. 1996, *A&AS*, **117**, 393, [1996A&AS..117..393B](#)
- Bertin, E. 2006, *Astronomical Data Analysis Software and Systems XV*, 112, [2006ASPC..351..112B](#)
- Bessell, M. S. 1979, *PASP*, **91**, 589, [1979PASP...91..589B](#)
- Bessell, M. S., & Brett, J. M. 1988, *PASP*, **100**, 1134, [1988PASP..100.1134B](#)
- Gaia DR2 Documentation 2019, <https://gea.esac.esa.int/archive/documentation/GDR2/>
- Gaia Collaboration, Brown, A. G. A., Vallenari, A., et al. 2018, *A&A*, **616**, A1, [2018A&A...616A...1G](#)
- Gaia EDR3, CDS catalog I/350.
- Iwanek, P., Soszyński, I., Kozłowski, S., et al. 2022, arXiv:2203.16552, [2022arXiv220316552I](#)
- Jester, S., Schneider, D. P., Richards, G. T., et al. 2005, *AJ*, **130**, 873, [2005AJ....130..873J](#)
- Jordi, K., Grebel, E. K., & Ammon, K. 2006, *A&A*, **460**, 339, [2006A&A...460..339J](#)
- Kato, T. 2001, *Information Bulletin on Variable Stars*, 5137, 1, [2001IBVS.5137....1K](#)
- Lang, D., Hogg, D. W., Mierle, K., et al. 2010, *AJ*, **139**, 1782, [2010AJ....139.1782L](#)
- Laycock, S., Tang, S., Grindlay, J., et al. 2010, *AJ*, **140**, 1062, [2010AJ....140.1062L](#)
- Lebzelter, T. 2011, *Astronomische Nachrichten*, **332**, 140, [2011AN....332..140L](#)
- Lenz, P., & Breger, M. 2005, *Communications in Asteroseismology*, 146, 53, [2005CoAst.146...53L](#)
- Maffei, P. 1975, *Information Bulletin on Variable Stars*, 985, 1, [1975IBVS..985....1M](#)
- Maffei, P., & Tosti, G. 1995, *AJ*, 109, 2652, [1995AJ....109.2652M](#)
- Maffei, P., & Tosti, G. 2013, *VizieR Online Data Catalog*, II/320, [2013yCat.2320....0M](#)
- Molnár, L., Joyce, M., & Kiss, L. L. 2019, *ApJ*, **879**, 62, [2019ApJ...879...62M](#)
- Nesci, R., Tuvikene, T., Rossi, C., et al. 2018, *Revista Mexicana de Astronomía y Astrofísica*, 54, 341, [2018RMxAA..54..341N](#)
- Nesci, R. 2018, *Information Bulletin on Variable Stars*, 6255, 1, [2018IBVS.6255....1N](#)
- Paunzen, E. & Vanmunster, T. 2016, *Astronomische Nachrichten*, 337, 239, [2016AN....337..239P](#)

- Press, W. H., & Rybicki, G. B. 1989, *ApJ*, 338, 277, [1989ApJ...338..277P](#)
- Reid, M. J., Menten, K. M., Brunthaler, A., et al. 2014, *ApJ*, **783**, 130, [1989ApJ...338..277P](#)
- Sabin, L., & Zijlstra, A. A. 2006, *MemSAIt*, **77**, 933, [2006MmSAI..77..933S](#)
- Scargle, J. D. 1982, *ApJ*, **263**, 835, [1982ApJ...263..835S](#)
- Schlegel, D. J., Finkbeiner, D. P., & Davis, M. 1998, *ApJ*, **500**, 525, [1998ApJ...500..525S](#)
- Soszyński, I., Udalski, A., Szymański, M. K., et al. 2011, *AcA*, **61**, 217, [2011AcA....61..217S](#)
- Soszyński, I., Udalski, A., Szymański, M. K., et al. 2009, *AcA*, **59**, 239, [2009AcA....59..239S](#)
- Soszyński, I., Udalski, A., Szymański, M. K., et al. 2013, *AcA*, **63**, 21, [2013AcA....63...21S](#)
- Schwarzenberg-Czerny, A., 1996, *ApJ*, **460**, L107-110, [1996ApJ...460L.107S](#)
- Templeton, M. R., Mattei, J. A., & Willson, L. A. 2005, *AJ*, **130**, 776, [2005AJ....130..776T](#)
- Tisserand, P. 2012, *A&A*, **539**, A51, [2012A&A...539A..51T](#)
- Tisserand, P., Clayton, G. C., Welch, D. L., et al. 2013, *A&A*, 551, A77, [2013A&A...551A..77T](#)
- Tuvikene, T., Edelmann, H., Groote, D., et al. 2014, *Astroplate 2014*, p. 127, [2014aspl.conf..127T](#)
- Udalski, A., Szymański, M. K., & Szymański, G. 2015, *AcA*, 65, 1, [2015AcA....65....1U](#)
- Walker, M. F. 1961, *ApJ*, **133**, 438, [1961ApJ...133..438W](#)
- Whitelock, P. A. 2012, *Ap&SS*, **341**, 123, [2012Ap&SS.341..123W](#)

SIMBAD	2MASS	OCVS	Maffei	Period	err	T0	Magmax	Magmin
FZ_Ser	18080193-1444151	OGLE-BLG-LPV-258610	M173	243.1	0.4	56939	12.5	15.7
GG_Ser	18081103-1434279	OGLE-BLG-LPV-258664	M101	362.2	0.8	56879	10.8	12.2
GH_Ser	18082202-1524048	OGLE-BLG-LPV-258711	M030	276.3	0.5	56917	12.1	14.2
GI_Ser	18082639-1535119	OGLE-BLG-LPV-258733	M090	252.1	0.5	56963	11.2	14.1
GK_Ser	18082549-1418077	OGLE-BLG-LPV-258729	M103	373.1	0.4	57123	13.6	16.1
GL_Ser	18083439-1507387	OGLE-BLG-LPV-258777	M031	171.2	0.2	56963	12.6	15.8
GM_Ser	18083581-1504017	BLG766.05.11	M092	193.8	0.8	57006	10.6	11.7
GN_Ser	18084003-1509393	OGLE-BLG-LPV-258806	M032	273.4	0.4	57060	12.0	15.3
GO_Ser	18085193-1408331	OGLE-BLG-LPV-258863	M003	237.3	0.4	57028	12.3	15.2
GP_Ser	18090980-1551201	OGLE-BLG-LPV-258945	M163	288.2	0.4	57058	12.1	14.9
GQ_Ser	18091802-1438126	OGLE-BLG-LPV-258994	M100	490.5	0.6	56969	12.5	15.8

GR_Ser	18092439-1519364	BLG767.28.8	M164	234.9	0.7	56950	9.4	16.0
GS_Ser	18092910-1407529	OGLE-BLG-LPV-259041	M020	373.9	0.3	57138	13.4	15.8
GT_Ser	18093492-1426408	OGLE-BLG-LPV-259071	M104	330.1	1.2	57119	13.3	16.6
GU_Ser	18093953-1455390	OGLE-BLG-LPV-259090	M002	330.2	1.5	57083	12.6	16.1
GV_Ser	18095709-1420456	OGLE-BLG-LPV-259169	M019	237.0	0.2	57002	13.4	15.3
GW_Ser	18095980-1451159	OGLE-BLG-LPV-259183	M105	296.8	0.5	56984	11.9	14.0
GX_Ser	18100565-1514019	OGLE-BLG-LPV-259204	M001	190.0	0.4	57016	10.6	13.1
GZ_Ser	18102342-1522234	OGLE-BLG-LPV-259281	M033	329.6	1.0	56885	10.9	13.9
HH_Ser	18102941-1507575	OGLE-BLG-LPV-259302	M042	490.3	1.0	57332	11.5	14.8
HI_Ser	18102813-1426061	OGLE-BLG-LPV-259297	M177	120.5	0.1	56869	12.3	15.7
HK_Ser	18104075-1352176	BLG766.27.8933	M050	446.0	0.0	40464	12.5	13.9
HL_Ser	18105937-1426022	OGLE-BLG-LPV-259454	M004	369.4	0.7	57159	12.8	14.9
HM_Ser	18110188-1535566	OGLE-BLG-LPV-259470	M034	197.5	0.2	57012	11.7	13.9
HN_Ser	18111261-1545228	OGLE-BLG-LPV-259535	M167	333.2	2.4	56942	12.7	16.3
HP_Ser	18112364-1537321	OGLE-BLG-LPV-259581	M093	478.1	1.1	57079	12.2	15.2
HQ_Ser	18113340-1544212	OGLE-BLG-LPV-259643	M094	314.1	0.7	57125	12.7	15.8
HR_Ser	18113915-1447054	OGLE-BLG-LPV-259675	M106	429.4	2.1	57288	11.2	14.0
HS_Ser	18114344-1508563	OGLE-BLG-LPV-259699	M017	516.8	0.8	57340	10.8	13.9
HT_Ser	18114978-1537187	OGLE-BLG-LPV-259738	M098	472.2	2.0	57287	12.2	15.1
HU_Ser	18115480-1540129	OGLE-BLG-LPV-259767	M095	401.0	1.5	57014	11.8	14.9
HV_Ser	18115776-1539244	OGLE-BLG-LPV-259785	M040	523.4	1.4	57316	11.5	14.2
HW_Ser	18120707-1454509	OGLE-BLG-LPV-259830	M045	286.9	0.6	57104	11.1	14.4
HX_Ser	18120879-1444481	OGLE-BLG-LPV-259839	M049	215.6	0.5	56942	13.3	16.1
HY_Ser	18121704-1547221	OGLE-BLG-LPV-259880	M039	204.0	0.2	57011	11.2	13.9
HZ_Ser	18121649-1424381	OGLE-BLG-LPV-259874	M008	454.5	1.0	56959	12.0	15.7
II_Ser	18122008-1522443	OGLE-BLG-LPV-259900	M041	328.7	0.8	56928	12.8	15.5
IK_Ser	18122562-1545195	OGLE-BLG-LPV-259930	M038	335.4	0.7	56886	12.1	14.8
IL_Ser	18123403-1520574	OGLE-BLG-LPV-259965	M107	202.9	0.3	56894	13.1	15.1
IM_Ser	18125363-1446150	OGLE-BLG-LPV-260070	M176	195.0	0.4	57027	12.7	14.3
IN_Ser	18125971-1454306	OGLE-BLG-LPV-260102	M207	474.4	0.8	57194	12.4	15.9
IO_Ser	18142466-1531035	OGLE-BLG-LPV-260511	M018	386.9	0.9	57026	11.7	14.0
IP_Ser	18144622-1407105	OGLE-BLG-LPV-260602	M117	214.1	0.8	56970	10.7	13.5
IQ_Ser	18150079-1548166	OGLE-BLG-LPV-260662	M006	356.7	0.7	57023	14.5	17.1
IR_Ser	18150239-1433461	OGLE-BLG-LPV-260675	M056	192.4	0.4	56997	12.4	14.9
IS_Ser	18150248-1407502	OGLE-BLG-LPV-260676	M022	436.9	1.2	57074	11.9	14.7
IT_Ser	18151980-1308503	OGLE-BLG-LPV-260767	M062	522.1	1.7	57396	12.5	15.6
IU_Ser	18152445-1402071	OGLE-BLG-LPV-260784	M181	372.2	1.1	57196	12.9	15.9
IV_Ser	18152657-1250317	OGLE-BLG-LPV-260794	M131	374.5	0.7	57202	13.2	15.8
IX_Ser	18153810-1505332	OGLE-BLG-LPV-260841	M179	301.9	0.8	56930	13.8	17.7
IY_Ser	18160250-1518028	OGLE-BLG-LPV-260944	M180	465.0	0.3	57279	12.3	15.0
IZ_Ser	18160690-1458486	OGLE-BLG-LPV-260964	M178	314.8	1.1	57168	13.5	16.3
KK_Ser	18190511-1243207	OGLE-BLG-LPV-261762	M013	287.0	0.7	57004	13.0	16.0
KM_Ser	18164727-1314374	OGLE-BLG-LPV-261136	M129	461.0	0.9	57229	12.7	16.0
KN_Ser	18165790-1553252	OGLE-BLG-LPV-261177	M110	350.8	0.5	57142	13.0	15.7

KO_Ser	18170085-1518195	OGLE-BLG-LPV-261194	M007	286.5	0.8	56934	10.5	13.6
KP_Ser	18173587-1239199	OGLE-BLG-LPV-261359	M194	242.6	0.8	56997	12.3	15.2
KQ_Ser	18175796-1304519	OGLE-BLG-LPV-261483	M189	294.7	0.4	57150	13.2	16.0
KR_Ser	18181305-1210243	OGLE-BLG-LPV-261546	M141	395.9	0.4	57046	12.1	14.0
KS_Ser	18181494-1227070	OGLE-BLG-LPV-261558	M142	411.5	0.6	56960	12.1	14.6
KT_Ser	18184060-1444469	OGLE-BLG-LPV-261660	M122	389.1	0.7	56928	10.8	13.6
KU_Ser	18190828-1447427	OGLE-BLG-LPV-261772	M009	451.1	3.0	56993	12.3	15.9
KV_Ser	18192266-1223526	OGLE-BLG-LPV-261824	M143	418.9	0.7	57237	12.4	14.8
KW_Ser	18193642-1439294	OGLE-BLG-LPV-261879	M121	223.3	0.4	57039	10.8	12.1
KX_Ser	18193773-1234294	OGLE-BLG-LPV-261886	M144	434.8	1.9	56939	12.4	15.8
KY_Ser	18195866-1236145	OGLE-BLG-LPV-261977	M081	324.3	1.5	56885	11.8	14.5
KZ_Ser	18200040-1309422	OGLE-BLG-LPV-261988	M140	511.9	2.5	57302	15.2	18.4
LM_Ser	18201740-1309171	OGLE-BLG-LPV-262058	M139	419.8	0.6	56936	13.6	16.1
LN_Ser	18203823-1332474	OGLE-BLG-LPV-262154	M190	189.7	0.4	57051	12.6	14.5
LO_Ser	18203583-1208358	OGLE-BLG-LPV-262143	M082	305.9	0.7	56925	12.3	15.6
LP_Ser	18204489-1228399	OGLE-BLG-LPV-262177	M148	256.8	1.1	57065	12.6	15.5
LQ_Ser	18204589-1252469	OGLE-BLG-LPV-262180	M197	394.4	0.5	57103	12.7	15.8
LR_Ser	18212341-1541420	OGLE-BLG-LPV-262341	M118	240.4	0.4	57059	12.9	15.8
NSV_10249	18082415-1535166	OGLE-BLG-LPV-258722	M091	191.4	0.2	56956	13.4	15.0
NSV_10271	18091451-1429483	OGLE-BLG-LPV-258970	M174	300.3	1.0	57274	13.1	16.8
NSV_10326	18110050-1423082	BLG766.18.154	M005	314.8	0.9	57130	14.1	16.3
NSV_10394	18140763-1506343	OGLE-BLG-LPV-260424	M021	310.0	0.8	57162	13.8	16.4
NSV_10408	18144139-1503536	OGLE-BLG-LPV-260585	M051	294.0	0.3	57105	13.7	16.4
NSV_10497	18173619-1502250	BLG779.06.3	M114	4.1	0.0	0	10.7	12.1
NSV_10522	18182915-1725379	OGLE-BLG-LPV-261605	M035	455.8	0.7	0	14.2	18.6
NSV_10677	18213621-1242312	OGLE-BLG-LPV-262404	M028	393.8	0.9	56956	14.0	16.6
NSV_10681	18214295-1300424	BLG778.17.9009	M159	1.8	0.0	0	13.4	14.8
NSV_10693	18215979-1634071	BLG569.16.43	M111	0.0	0.0	0	14.1	15.6
NSV_10772	18254743-1611475	BLG569.19.104	M183	262.2	1.3	56910	13.5	13.9
NSV_10832	18274962-1343087	BLG574.06.26871	M087	326.7	1.5	57071	11.3	12.5
NSV_10899	18295552-1518384	OGLE-BLG-T2CEP-1311	M024	68.1	0.0	0	12.6	13.8
V374_Sct	18230920-1237573	BLG787.23.49	M203	421.4	1.6	57028	13.4	14.8
V375_Sct	18231684-1301356	BLG787.06.9360	M147	512.3	4.0	57330	13.3	16.3
V377_Sct	18245921-1418133	OGLE-BLG-LPV-263346	M071	514.3	1.6	56941	11.7	16.3
V379_Sct	18252234-1531597	OGLE-BLG-LPV-263451	M010	412.4	0.9	57028	11.3	14.6
V380_Sct	18254033-1443006	OGLE-BLG-LPV-263528	M138	443.9	1.8	57086	12.1	15.0
V381_Sct	18255250-1532074	BLG789.01.34839	M188	395.8	1.4	57054	12.6	14.5
V382_Sct	18260817-1447151	OGLE-BLG-LPV-263639	M069	563.6	1.2	57463	10.6	13.3
V383_Sct	18263656-1550387	OGLE-BLG-LPV-263764	M061	295.5	0.3	57068	12.6	15.3
V384_Sct	18265495-1540225	OGLE-BLG-LPV-263846	M128	461.7	0.6	57027	12.8	16.2
V386_Sct	18271563-1549354	OGLE-BLG-LPV-263898	M026	472.4	1.0	57204	11.5	14.5
V387_Sct	18271547-1532243	OGLE-BLG-LPV-263897	M063	387.0	1.8	57179	12.2	14.8
V388_Sct	18273471-1338110	OGLE-BLG-LPV-263951	M204	372.6	0.5	44374	10.8	14.2
V389_Ser	18083617-1447341	OGLE-BLG-LPV-258786	M172	236.9	0.4	57097	13.2	16.0

V390_Ser 18090604-1518371 OGLE-BLG-LPV-258926 M165 170.8 0.6 57018 11.5 13.2
V3904_Sgr 18110608-1613039 OGLE-BLG-LPV-259494 M089 356.8 0.7 57015 11.4 15.6
V3905_Sgr 18111338-1603290 OGLE-BLG-LPV-259541 M162 319.9 0.4 56911 13.3 19.7
V391_Sct 18280661-1554440 BLG576.14.26 M064 0.0 0.0 0 11.7 15.7
V391_Ser 18095802-1458356 OGLE-BLG-LPV-259174 M099 245.1 0.3 57022 12.0 15.1
V3918_Sgr 18290441-1353350 OGLE-BLG-LPV-264248 M086 401.8 1.2 57027 11.3 14.4
V392_Sct 18281253-1514385 OGLE-BLG-LPV-264078 M193 484.8 0.7 57346 12.8 15.3
V3920_Sgr 18173387-1732054 OGLE-BLG-LPV-261345 M088 465.5 0.2 57029 12.3 15.6
V3921_Sgr 18173623-1741404 OGLE-BLG-LPV-261362 M029 528.5 1.7 57043 12.8 15.7
V3924_Sgr 18192768-1745477 OGLE-BLG-LPV-261845 M096 362.8 1.2 57238 12.7 14.9
V3925_Sgr 18193309-1746442 OGLE-BLG-LPV-261863 M037 152.1 0.2 56898 11.0 16.2
V3926_Sgr 18193414-1748395 OGLE-BLG-LPV-261868 M168 285.6 0.5 57072 11.7 14.3
V3927_Sgr 18195744-1743099 OGLE-BLG-LPV-261965 M097 218.4 0.3 56895 11.5 14.1
V3930_Sgr 18210828-1706231 OGLE-BLG-LPV-262275 M108 432.3 1.3 57286 13.0 17.1
V3931_Sgr 18212174-1642586 OGLE-BLG-LPV-262339 M048 439.7 0.5 57027 11.7 14.9
V3932_Sgr 18214251-1732069 OGLE-BLG-LPV-262446 M047 204.4 0.2 56971 11.2 13.4
V3934_Sgr 18230629-1721099 OGLE-BLG-LPV-262824 M109 187.1 0.4 57043 12.8 14.6
V3935_Sgr 18240935-1703399 OGLE-BLG-LPV-263102 M052 403.6 1.0 57185 12.8 15.6
V3936_Sgr 18241836-1707212 OGLE-BLG-LPV-263146 M112 376.1 1.8 57221 12.9 14.3
V3938_Sgr 18243941-1705018 OGLE-BLG-LPV-263241 M054 294.5 0.5 57129 11.5 14.4
V394_Sct 18281864-1525508 OGLE-BLG-LPV-264107 M066 311.2 1.3 57099 11.2 14.7
V394_Ser 18135798-1521596 OGLE-BLG-LPV-260384 M046 326.9 0.4 57174 13.4 16.4
V3940_Sgr 18250931-1636201 OGLE-BLG-LPV-263393 M057 451.5 2.3 57183 10.3 17.8
V3942_Sgr 18253922-1633460 OGLE-BLG-LPV-263526 M120 357.5 2.0 56930 10.1 13.3
V3943_Sgr 18264699-1557304 OGLE-BLG-LPV-263811 M123 367.2 0.7 57005 12.3 15.5
V3944_Sgr 18264776-1621427 OGLE-BLG-LPV-263813 M058 294.4 1.1 56900 12.7 16.0
V3945_Sgr 18272269-1615389 OGLE-BLG-LPV-263921 M023 317.4 1.2 56984 11.1 14.4
V3946_Sgr 18274130-1621546 OGLE-BLG-LPV-263978 M059 405.2 1.4 57264 12.4 14.8
V3947_Sgr 18274739-1607056 OGLE-BLG-LPV-263995 M060 308.1 0.7 56907 10.7 13.7
V3949_Sgr 18281973-1621109 OGLE-BLG-LPV-264113 M126 501.0 2.1 56867 11.2 13.3
V395_Sct 18282052-1506009 OGLE-BLG-LPV-264116 M074 314.1 1.5 56913 11.7 14.5
V3950_Sgr 18283838-1603253 BLG576.05.34937 M127 199.0 0.4 56970 12.3 13.4
V396_Ser 18163239-1242177 OGLE-BLG-LPV-261077 M132 423.9 1.4 56907 14.4 18.4
V397_Sct 18283100-1519244 OGLE-BLG-LPV-264143 M068 318.3 0.6 56881 11.8 15.1
V397_Ser 18164368-1551070 BLG780.16.28126 M175 237.9 0.7 56890 12.5 13.2
V398_Sct 18283358-1456333 OGLE-BLG-LPV-264150 M145 183.3 0.4 56945 12.5 14.4
V398_Ser 18164590-1341174 OGLE-BLG-LPV-261132 M186 319.9 1.5 57022 13.8 16.9
V399_Sct 18283523-1456186 OGLE-BLG-LPV-264162 M075 322.3 1.3 57180 11.9 14.8
V400_Sct 18284236-1522525 OGLE-BLG-LPV-264184 M067 294.1 0.5 57138 11.1 12.5
V400_Ser 18174215-1434567 OGLE-BLG-LPV-261390 M182 426.4 0.7 57133 13.2 16.1
V401_Sct 18285417-1429201 OGLE-BLG-LPV-264225 M080 485.0 1.3 57071 10.7 13.4
V402_Ser 18190905-1242465 OGLE-BLG-LPV-261780 M070 318.4 1.6 56991 14.1 17.4
V403_Sct 18290273-1446582 OGLE-BLG-LPV-264241 M198 333.5 0.8 56956 12.1 14.8
V404_Sct 18291283-1537377 OGLE-BLG-LPV-264281 M065 282.3 0.3 57090 12.6 15.6

V404_Ser	18184746-1237123	OGLE-BLG-LPV-261696	M012	341.6	1.1	57108	12.2	14.4
V405_Sct	18292248-1507598	OGLE-BLG-LPV-264309	M015	355.2	0.7	56879	12.5	15.4
V407_Sct	18293219-1548396	OGLE-BLG-LPV-264335	M135	234.4	0.3	56910	9.9	13.1
V408_Sct	18293898-1446124	BLG575.12.937	M201	321.8	0.0	57357	12.4	15.6
V410_Sct	18295301-1457534	OGLE-BLG-LPV-264383	M199	322.9	1.0	56916	12.4	14.6
V411_Sct	18275904-1343220	OGLE-BLG-LPV-264039	M208	454.0	1.6	57312	11.2	13.4
V412_Sct	18295881-1410102	OGLE-BLG-LPV-264401	M152	412.0	1.5	57019	12.9	15.3
V413_Sct	18300233-1528300	OGLE-BLG-LPV-264415	M136	334.9	1.4	57069	12.7	15.6
V414_Sct	18301384-1527224	OGLE-BLG-LPV-264442	M137	546.7	1.8	41240	13.6	16.8
V415_Sct	18301342-1425191	OGLE-BLG-LPV-264440	M084	302.0	0.8	57092	10.5	14.6
V416_Sct	18301476-1421339	OGLE-BLG-LPV-264443	M205	300.3	0.7	57052	11.1	14.7
V417_Sct	18301572-1431265	OGLE-BLG-LPV-264445	M202	405.5	1.2	57231	10.1	12.8
V418_Sct	18302897-1421353	OGLE-BLG-LPV-264484	M154	399.1	2.9	56871	11.4	13.4
V419_Sct	18303629-1416248	OGLE-BLG-LPV-264499	M153	364.5	0.6	57192	12.1	14.8
V420_Sct	18304816-1452459	OGLE-BLG-LPV-264532	M085	257.0	0.4	57089	10.0	12.5
V421_Sct	18305093-1537289	OGLE-BLG-LPV-264539	M076	218.5	0.8	56959	11.2	14.6
V422_Sct	18312526-1518226	OGLE-BLG-LPV-264637	M078	406.6	1.0	57141	12.3	15.0
V423_Sct	18312523-1443501	OGLE-BLG-LPV-264636	M206	453.4	0.8	56952	12.1	14.7
V424_Sct	18313627-1526581	OGLE-BLG-LPV-264672	M077	473.5	1.0	57244	11.4	14.4
V425_Sct	18314233-1512142	OGLE-BLG-LPV-264693	M200	451.4	3.8	57170	11.3	14.3
V478_Sct	18241283-1315552	OGLE-BLG-LPV-263121	M083	506.5	2.2	57379	13.2	17.4
V5536_Sgr	18250499-1703578	OGLE-BLG-LPV-263376	M113	206.7	0.5	57057	13.1	16.5